Direct Additive Detection in Polymer Films via Platinum-Assisted SALDI Mass Spectrometry Imaging

Hideya Kawasaki[*,1], Issey Osaka[2], and Ryuichi Arakawa[1]

[1]Department of Chemistry and Materials Engineering, Kansai University, 3–3–35 Yamate-cho, Suita, Osaka 564–8680, Japan
[2]Department of Pharmaceutical Engineering, Faculty of Engineering, Toyama Prefectural University, 5180 Kurokawa, Imizu-City, Toyama 939–0398, Japan

In this study, we employed platinum-assisted surface-assisted laser desorption/ionization mass spectrometry imaging (MSI) (Pt-SALDI-MSI) to detect and visualize the spatial distribution of antioxidant additives and organic dyes in polystyrene films undergoing photodegradation. In traditional matrix-assisted laser desorption/ionization mass spectrometry (MALDI-MS), matrix-derived ion peaks often obscure signals from low-molecular-weight analytes. Pt-SALDI-MSI, which utilizes inorganic nanoparticles instead of an organic matrix, enables the interference-free analysis of low-molecular-weight compounds, thereby addressing the limitation of traditional MALDI-MS. Using Pt-SALDI-MSI, we observed the degradation and distribution of Irganox 1098 (an antioxidant) and crystal violet (an organic dye) following ultraviolet irradiation. This method effectively captures the photodegradation process, providing valuable insights into the environmental breakdown of plastics and the formation of microplastics.

1. INTRODUCTION

Matrix-assisted laser desorption/ionization mass spectrometry (MALDI-MS) is a widely used technique in mass spectrometry. One notable advantage of this technique is that the matrix absorbs most of the laser energy, preventing sample decomposition and enabling high-sensitivity detection of high-molecular-weight compounds such as peptides and proteins.[1] However, a significant limitation remains: the matrix desorbs and ionizes along with the sample, producing strong interfering ion peaks in the low-molecular-weight region of the mass spectrum. This interference makes it challenging to analyze low-molecular-weight compounds accurately.[2]

To address this issue, surface-assisted laser desorption/ionization mass spectrometry (SALDI-MS) was developed as a matrix-free ionization technique. SALDI-MS employs inorganic nanoparticles as ionization-assisting agents, thereby avoiding matrix-derived ion peaks and facilitating the interference-free analysis of low-molecular-weight compounds.[3–5] Among the various inorganic nanoparticles, platinum (Pt) has shown particular efficacy as an ionization-assisting agent in SALDI-MS owing to its favorable properties, including ultraviolet (UV) light absorption, high melting point, good electrical conductivity, and low thermal conductivity.[6–10]

Mass spectrometry imaging (MSI) has been applied to biological samples using MALDI-MS. MSI performs mass spectrometry on entire tissue sections, producing images that show the spatial distribution of specific ion peaks.[11] Although MSI is typically conducted with MALDI-MS, it has certain limitations, such as uneven matrix distribution ("sweet spots") and positional inaccuracies caused by solvent effects.[12] To overcome these limitations in MALDI-MSI, SALDI-based MSI has been developed recently.[13,14] Our group has developed a Pt-deposited SALDI-MS (Pt-SALDI-MSI) for MSI applications.[15–18] Pt-SALDI-MSI provides a more uniform coating of samples via Pt deposition, reduces sample misalignment due to its dry deposition process, and is suitable for analyzing non-conductive samples.

*Correspondence to: Hideya Kawasaki, *Department of Chemistry and Materials Engineering, Kansai University, 3–3–35 Yamate-cho, Suita, Osaka 564–8680, Japan*, e-mail: hkawa@kansai-u.ac.jp

Synthetic polymer chemistry has advanced significantly over the past century, leading to diverse macromolecules with complex structures. Mass spectrometry has become a key tool in analyzing these polymers, especially in addressing challenges like desorption, ionization, and structural analysis of large molecules while reducing spectral complexity.[19–21] Analyzing the additives in polymers and plastic materials is essential for understanding the distribution of these substances in polymer-based products. Additives are incorporated into polymers to enhance their durability, UV protection, and color stability, among other characteristics. The types and proportions of these additives vary depending on the processing method, application, and manufacturer, making their analysis crucial for quality control and performance optimization. Traditional extraction-based methods for polymer additive analysis, such as gas chromatography and high-performance liquid chromatography, are commonly used to separate and quantify volatile and nonvolatile organic additives.[22–24] Although effective for identifying and quantifying these components, these methods are limited in their ability to visualize the spatial distribution of additives within the material and their changes over time. Therefore, complementary analytical methods such as Fourier-transform infrared spectroscopy (FT-IR) and X-ray photoelectron spectroscopy (XPS) are often employed. However, FT-IR and XPS primarily provide information on functional groups and molecular structures rather than a detailed spatial distribution.

The SALDI-MSI allows for the analysis of non-conductive samples and is particularly effective in detecting low-molecular-weight compounds. This technique shows promise as a direct method for identifying and mapping the distribution of additives within polymer matrices. Despite its potential, studies on the application of SALDI-MSI for additive analysis in polymers remain scarce.[25] In this study, we used Pt-SALDI-MSI to detect and investigate the spatial distribution of additives, particularly antioxidant additives and organic dyes, in polystyrene films. Understanding the degradation behavior of antioxidants under UV irradiation is essential to elucidate their protective role in polymer films and assess their effectiveness in preventing degradation. UV degradation is one of the primary mechanisms whereby plastics decompose in the environment.[26–28] Plastics containing additives deteriorate progressively under UV exposure, generating small fragments and fine particles. These microplastic fragments accumulate in the environment, raising concerns about their entry into rivers and oceans. Therefore, we examined the transformation of the additives into polystyrene films subjected to UV irradiation using Pt-SALDI-MSI.

2. EXPERIMENTAL

2.1 Reagents

Sodium trifluoroacetate (NaTFA), angiotensin II (Ang II), dimethyl[4-[bis[4-(dimethylamino)phenyl]methylene]-2,5-cyclohexadiene-1-ylidene]aminium chloride (crystal violet; CV), and tetrahydrofuran (THF) were purchased from Wako Pure Chemical Industries, Ltd. (Osaka, Japan) Polystyrene and α-cyano-4-hydroxycinnamic acid (CHCA) were obtained from Sigma-Aldrich (Burlington, MA, USA). Ethyl 3,5-di-tert-butyl-4-hydroxybenzylphosphonic acid (Irganox 1098) and

tris(2,4-di-tert-butylphenyl)phosphite (Irgafos 168) was sourced from Ciba Specialty Chemicals Co., Ltd. (Basel, Switzerland).

2.2 Pt-SALDI-MS measurement of additives in polystyrene film

2.2.1 Polystyrene film with Irganox 1098 and Irgafos 168

The polystyrene films containing additives were prepared by dissolving polystyrene in THF with 1% (w/w) Irganox 1098 and 1% (w/w) Irgafos 168. This solution was then spin-coated onto a substrate to form uniform films, using 300 μL of the solution at a rotation speed of 300 rpm for 30 s, and the film was deposited onto a glass substrate. Pt was deposited on the polymer film to a thickness of 10 nm, and SALDI-MS measurements were conducted. In addition, one of the films was exposed to UV light for 20 min using a high-pressure mercury lamp.

2.2.2 Polystyrene film with CV

A solution of polystyrene in THF was mixed with 0.5 wt% CV. This solution was spin-coated to form uniform films by applying 300 μL at 300 rpm for 30 s, and the polymer film was deposited onto a glass substrate. Hereafter, the polymer films were exposed to UV light for 10, 20, or 30 min using a high-pressure mercury lamp. Pt was deposited on all the films, including one that was not exposed to UV light, at a thickness of 10 nm. Subsequently, Pt-SALDI-MS measurements were performed.

2.2.3 Instrumentation

SALDI-MS was performed in the positive-ion mode using an AXIMA-CFR mass spectrometer (Shimadzu Corporation, Kyoto, Japan). Calibration was conducted with CHCA and Ang II H$^+$ adducts, detected at m/z 190.05 and m/z 1046.54, respectively. SALDI-MSI measurements were performed using an Autoflex Speed instrument (Bruker Daltonics, Bremen, Germany). UV exposure was applied using a high-pressure mercury lamp (HLR100T-2, Mizuka Planning Co., Ltd., Tokyo, Japan) with a UV intensity of 170 W/cm². Pt was deposited using an MSP-1S magnetron sputtering device (Vacuum Device Inc., Ibaraki, Japan) and a JFC-1600 sputter coater (JEOL Ltd., Tokyo, Japan). The NaTFA cationizing agent solution (0.5 mg/mL) was sprayed using a Mr. Linear Compressor L5 (GSI Creos Corporation, Tokyo, Japan), and the spin coating was performed using an Opticoat MS-A100 spin coater (Mikasa Co. Ltd., Tokyo, Japan).

3. RESULTS AND DISCUSSION

3.1 Antioxidants in polystyrene film

Irganox 1098 is a hindered phenol antioxidant that acts as a radical scavenger, while Irgafos 165 is a phosphite-based stabilizer that decomposes hydroperoxides, preventing oxidative degradation of polymers. Both are widely used to enhance the stability of polymers by addressing different aspects of degradation pathways.

Figure 1 shows the Pt-SALDI-MS mass spectra of polystyrene films containing various concentrations of Irganox 1098 (0.1, 1, and 5 wt%). In the film with 5 wt% Irganox 1098, peaks corresponding to Na$^+$ and K$^+$ adducts were observed,
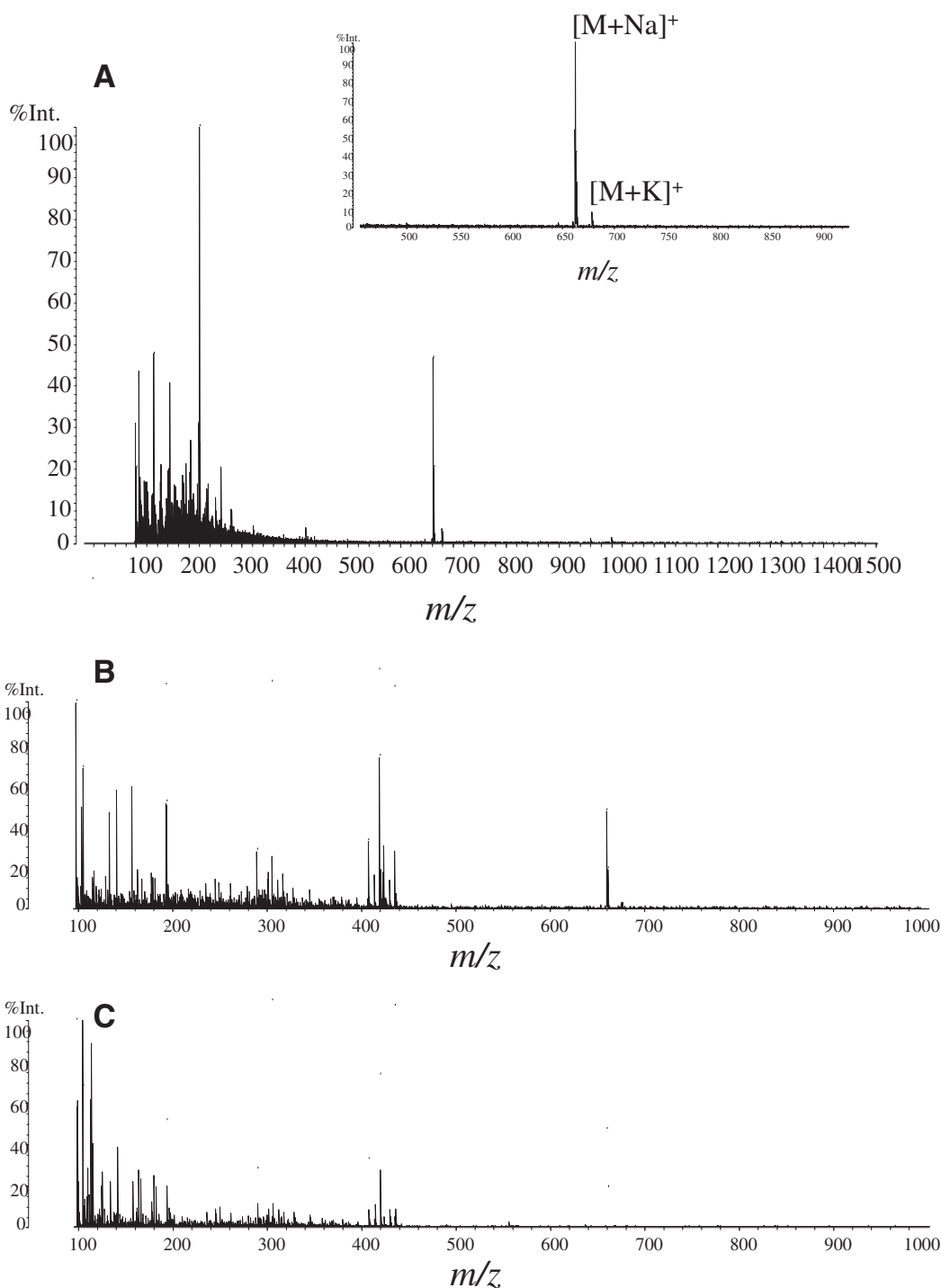
Fig. 1. Pt-SALDI-MS mass spectra of polystyrene films containing various concentrations of Irganox 1098 with (A) 5 wt%, (B) 1 wt%, and (C) 0.1 wt%. Pt-SALDI-MS, platinum-deposited surface-assisted laser desorption/ionization mass spectrometry.

with the Na$^+$ adduct peak showing greater intensity (Fig. 1A). When NaTFA cationizing agent solution is sprayed during analysis, the sodium ions detected as adducts are likely derived from this solution. Conversely, the detection of Irganox as potassium adduct ions indicates that K$^+$ likely originated either from the original sample or as a result of environmental contamination during the analysis. As the concentration of Irganox 1098 decreased, the Na$^+$ adduct peak intensity diminished, becoming less prominent at 1 wt% (Fig. 1B) and undetectable at 0.1 wt% (Fig. 1C). In the Pt-SALDI-MS spectrum of the polystyrene film containing

1 wt% Irgafos 168, a peak corresponding to the protonated molecule was detected (Fig. S1).

3.2 Photodegradation of antioxidants in polystyrene film

Figure 2 shows the Pt-SALDI-MS spectra of a polystyrene film containing 1 wt% each of Irganox 1098 and Irgafos 168 recorded before and after UV irradiation for 20 min. Prior to irradiation, only the Na$^+$ and K$^+$ adduct peaks of Irganox 1098 were detected and no peaks for Irgafos 168 were observed (Fig. 2A). This suggests an ion-suppression
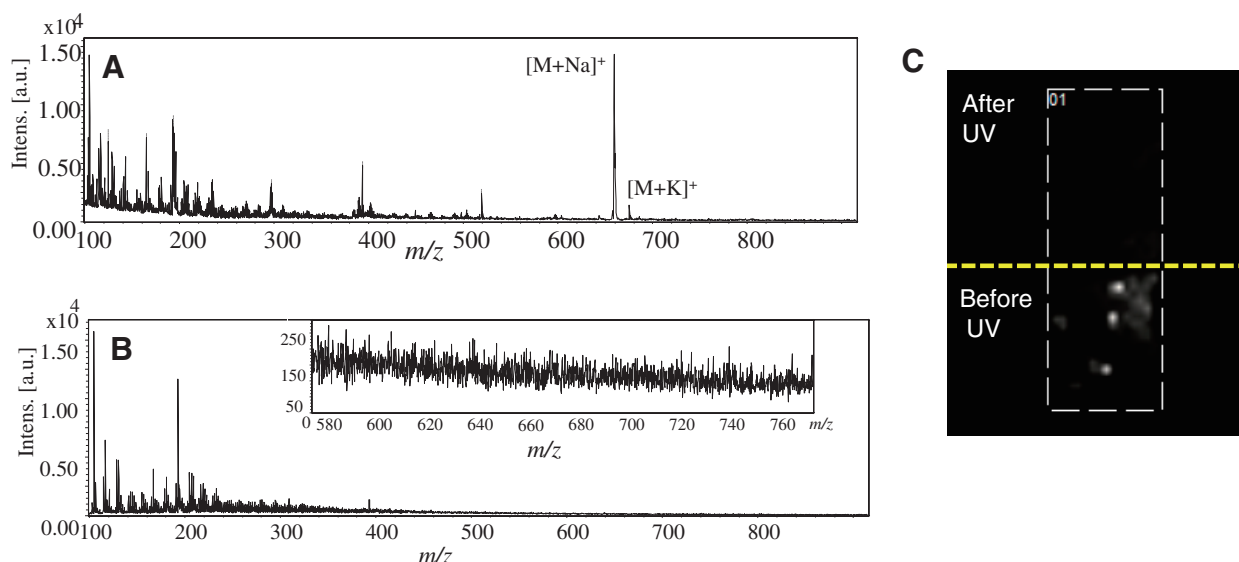
Fig. 2. Pt-SALDI-MS spectra of a polystyrene film containing 1 wt% Irganox 1098 and 1 wt% Irgafos 168 (A) before and (B) after UV irradiation. (C) Ion images of the polystyrene film containing 1 wt% Irganox 1098 and 1 wt% Irgafos 168 before and after UV irradiation using Pt-SALDI-MSI (the Na$^+$ adduct of Irganox 1098 at m/z 660 ± 3.3, laser interval: 100 μm). Pt-SALDI-MS, platinum-deposited surface-assisted laser desorption/ionization mass spectrometry; Pt-SALDI-MSI, platinum-deposited surface-assisted laser desorption/ionization imaging mass spectrometry; UV, ultraviolet.

effect of Irgafos 168, which led to the preferential detection of Irganox 1098. After the UV exposure, the Irganox 1098 peak disappeared, indicating that Irganox 1098 underwent photodegradation (Fig. 2B). Figure 2C displays ion images of the polystyrene film containing 1 wt% Irganox 1098 and 1 wt% Irgafos 168, both before and after UV irradiation, using Pt-SALDI-MSI (Na$^+$ adduct at m/z 660 ± 3.3, laser interval: 100 μm). In this study, the laser interval of 100 μm represents the spacing between measurement points during laser scanning performed within the sample.

The spotty signal intensities observed in the non-irradiated regions, as shown in Fig. 2C, could indeed be due to the uneven distribution of additives in the polymer film. After irradiation, the Irganox 1098 peaks were no longer detectable in the UV-irradiated region, demonstrating that Pt-SALDI-MSI can effectively monitor the photodegradation of Irganox 1098 in polystyrene films. Although the reduction of Irganox 1098 was clearly visualized, structural identification and imaging of its decomposition products were not achieved in this study.

3.3 Photodegradation of CV dye

CV dye was selected as a representative dye due to its ease of detection via mass spectrometry, enabling us to monitor the additive's distribution effectively. In addition, CV is commonly used to alter the optical properties of polymer films. CV dye was detected using LDI-MS without a Pt coating (Fig. S2a). However, with Pt-SALDI-MS, the peak intensity increased approximately 150-fold, with a prominent peak for CV [M$^+$] at m/z 372 (Fig. S2b), indicating that the Pt coating significantly enhanced the CV peak intensity. Figure 3 presents the Pt-SALDI-MS spectra of a polystyrene film containing 0.5 wt% CV before and after 10, 20, and 30 min of UV exposure. Following UV irradiation, peaks for the CV degradation products appeared, with low-molecular-weight fragments observed as the exposure time increased. These

degradation products were detected at m/z 358, 344, 330, and 316, along with a molecular ion at m/z 372. The chemical structures of the degradation products are shown in Fig. S3. After 30 min of irradiation, the original peak at m/z 372 was no longer detectable.

Figures 4 and 5 show ion images obtained by Pt-SALDI-MSI (laser interval: 300 μm) of the polystyrene film containing 0.5 wt% CV before and after 10 and 20 min of UV irradiation. In this study, the laser interval of 300 μm represents the spacing between measurement points during laser scanning performed within the sample. The integrated Pt-SALDI-MS mass spectra of Pt-SALDI-MSI are shown in Fig. S4. An optical photograph of the film post-UV exposure, with UV light applied through a custom slit and a high-pressure mercury lamp, shows faded coloration in the irradiated area (Fig. 4A). The ion images in Fig. 4 depict (B) the molecular ion of CV at m/z 372 ± 0.9 and degradation products at (C) m/z 358 ± 0.9, (D) m/z 344 ± 0.9, (E) m/z 330 ± 0.8, and (F) m/z 316 ± 0.8. After 20 min of UV exposure, the intensity of the CV molecular ion peak (m/z 372) decreased, whereas the peak at m/z 358 became indistinct, as shown in Fig. 5. The peaks at m/z 344, 330, and 316 became more pronounced, enabling visualization of the spatial distribution of the photodegraded CV products in the ion images. After 30 min of UV exposure, further degradation occurred and almost no detectable signal was observed in the UV-irradiated region (Fig. S5).

In this study, no polymer degradation products were detected; however, the detection and analysis of such products remain essential for achieving a deeper understanding of polymer degradation mechanisms. In addition, mass spectrometry imaging of photodegradation compounds derived from additives, such as antioxidants, is pivotal in exploring how these compounds affect the formation of polymer degradation products. This underscores the intricate relationship between additive photodegradation and
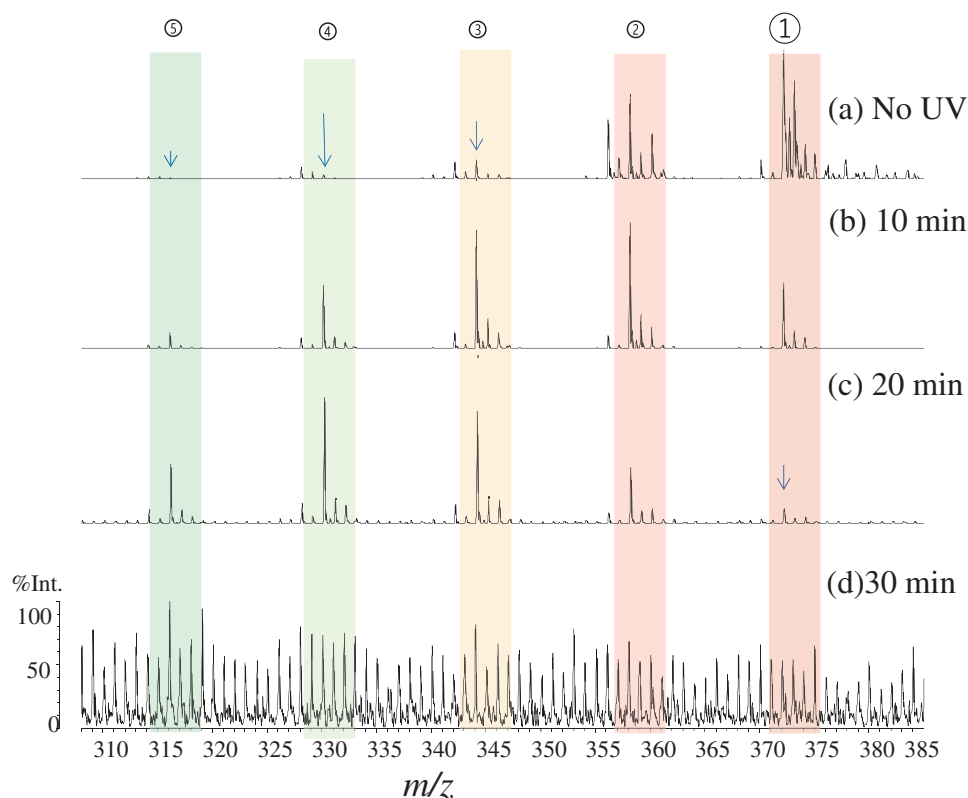
Fig. 3. Pt-SALDI-MS spectra of a polystyrene film containing 0.5 wt% CV dye before irradiation (No UV) and after 10, 20, and 30 minutes of UV exposure. Peaks from degradation products of the dye after UV exposure at m/z ②358, ③344, ④330, and ⑤316, besides the molecular ion at ①m/z 372. CV, crystal violet; Pt-SALDI-MS, platinum-deposited surface-assisted laser desorption/ionization mass spectrometry; UV, ultraviolet.
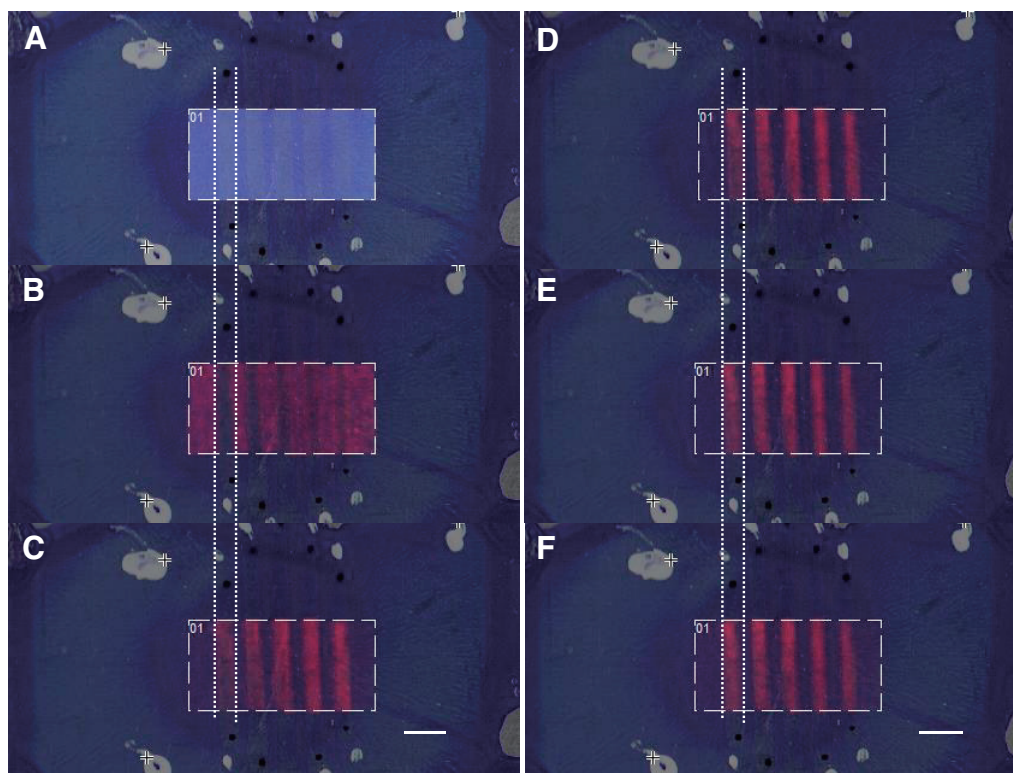

Fig. 4. Ion images obtained by Pt-SALDI-MSI (laser interval: 300 μm) for the polystyrene film containing 0.5 wt% CV after UV irradiation for 10 min (B)–(F). (B) m/z 372 ± 0.9, (C) m/z 358 ± 0.9, (D) m/z 344 ± 0.9, (E) m/z 330 ± 0.8, and (F) m/z 316 ± 0.8. The photograph of polystyrene film is also shown in (A). The contrast of the image inside the frame in (A) differs from that outside the frame because the image within the frame is a photograph of the sample, adjusted to enhance its visibility. The width of the slit is 2.0 mm. The scale bar is 4 mm. CV, crystal violet; Pt-SALDI-MSI, platinum-deposited surface-assisted laser desorption/ionization imaging mass spectrometry; UV, ultraviolet.
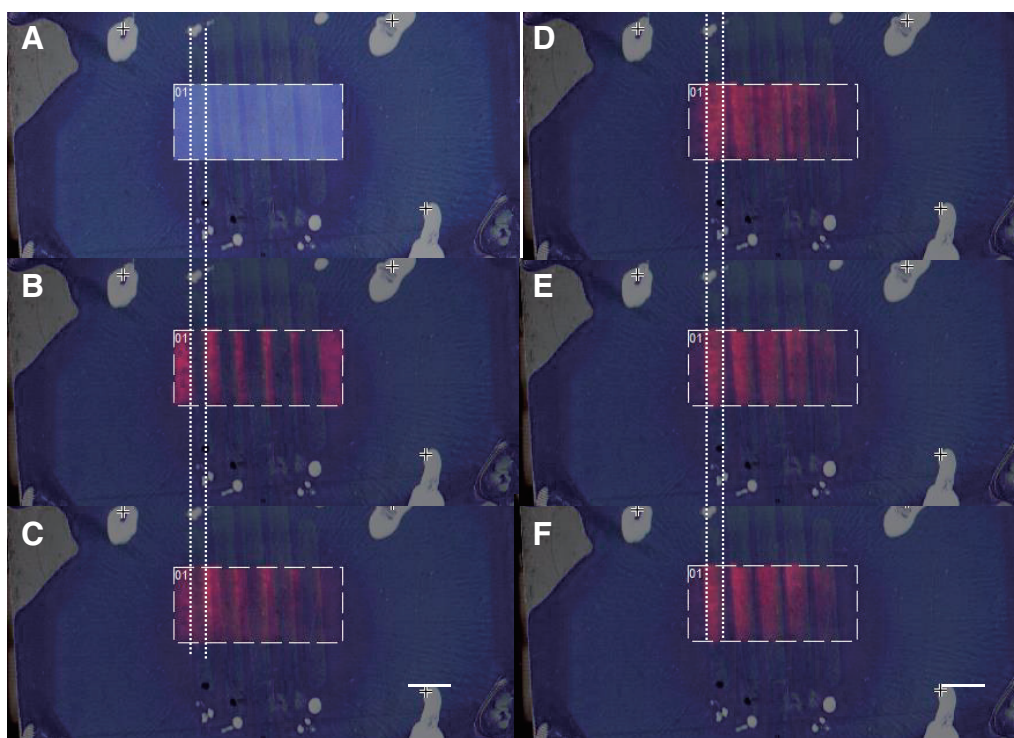
Fig. 5. Ion images obtained by Pt-SALDI-MSI (laser interval: 300 μm) for the polystyrene film containing 0.5 wt% CV after UV irradiation for 20 min (B)–(F). (B) m/z 372 ± 0. 9, (C) m/z 358 ± 0. 9, (D) m/z 344 ± 0. 9, (E) m/z 330 ± 0. 8, and (F) m/z 316 ± 0.8. The photograph of polystyrene film is also shown in (A). The contrast of the image inside the frame in (A) differs from that outside the frame because the image within the frame is a photograph of the sample, adjusted to enhance its visibility. The width of the slit is 2.0 mm, The scale bar is 4 mm. CV, crystal violet; Pt-SALDI-MSI, platinum-deposited surface-assisted laser desorption/ionization imaging mass spectrometry; UV, ultraviolet.

polymer stability, highlighting an important area for future research aimed at further elucidating the degradation pathways of polymers.

4. CONCLUSION

The Pt-SALDI-MSI technique demonstrated in this study proved effective for analyzing additives and their degradation in polystyrene films. The photodegradation of the antioxidant Irganox 1098 and the spatial distribution of the degradation products of CV dye were successfully visualized, confirming that Pt-SALDI-MSI enables the matrix-free analysis of low-molecular-weight compounds. This approach shows great potential for advancing our understanding of polymer degradation mechanisms and the environmental decomposition of plastics.

REFERENCES

1) K. Dreisewerd. The desorption process in MALDI. *Chem. Rev.* 103: 395–426, 2003.

2) Z. Sun, F. Wang, Y. Liu, B. Deng, R. Ren, Y. Wang, D. Chen, L. Zuo. Recent strategies for improving MALDI mass spectrometry imaging performance towards low molecular weight compounds. *Trends Analyt. Chem.* 175: 117727, 2024.

3) H. Sato, S. Nakamura, T. N. J. Fouquet, T. Ohmura, M. Kotani, Y. Naito. Simple pretreatment for the analysis of additives and polymers by surface-assisted laser desorption/ionization mass spectrometry using a through-hole alumina membrane as a functional substrate. *J. Am. Soc. Mass Spectrom.* 31: 298–307, 2020.

4) T. Kakuta, N. Manyuan, H. Kawasaki. UV-absorbing ligand capped gold nanoparticles for the SALDI-MS analysis of small molecules. *Mass Spectrom. (Tokyo)* 11: A0107, 2022.

5) W. Ma, J. Li, X. Li, Y. Bai, H. Liu. Nanostructured substrates as matrices for surface assisted laser desorption/ionization mass spectrometry: A progress report from material research to biomedical applications. *Small Methods* 5: 2100762, 2021.

6) H. Kawasaki, T. Yonezawa, T. Watanabe, R. Arakawa. Platinum nanoflowers for surface-assisted laser desorption/ionization mass spectrometry of biomolecules. *J. Phys. Chem. C Nanomater. Interfaces* 111: 16278–16283, 2007.

7) T. Yonezawa, H. Kawasaki, A. Tarui, T. Watanabe, R. Arakawa, T. Shimada, F. Mafuné. Detailed investigation on the possibility of nanoparticles of various metal elements for surface-assisted laser desorption/ionization mass spectrometry. *Anal. Sci.* 25: 339–346, 2009.

8) H. Kawasaki, T. Yao, T. Suganuma, K. Okumura, Y. Iwaki, T. Yonezawa, T. Kikuchi, R. Arakawa. Platinum nanoflowers on scratched silicon by galvanic displacement for an effective SALDI substrate. *Chemistry* 16: 10832–10843, 2010.

9) S. Nitta, H. Kawasaki, T. Suganuma, Y. Shigeri, R. Arakawa. Desorption/ionization efficiency of common amino acids in surface-assisted laser desorption/ionization mass spectrometry (SALDI-MS) with nanostructured platinum. *J. Phys. Chem. C Nanomater. Interfaces* 117: 238–245, 2013.

10) K. Hashimoto, K. Kaneda, T. Shimazaki, C. Kurihashi, S. Yamamoto, R. Takata, S. Nakanishi, I. Osaka. Effect of the surface morphology of a metal film on ion yields in a platinum-film surface-assisted laser desorption/ionization mass spectrometry. *Mass Spectrom. (Tokyo)* 13: A0154, 2024.

11) J. L. Moore, G. Charkoftaki. A guide to MALDI imaging mass spectrometry for tissues. *J. Proteome Res.* 22: 3401–3417, 2023.

12) A. A. Patil, M. J. N. Descanzo, V. B. Dhisale, W.-P. Peng. MALDI sample preparation methods: A mini review. *Int. J. Mass Spectrom.* 498: 117219, 2024.

13) W. H. Müller, A. Verdin, E. De Pauw, C. Malherbe, G. Eppe. Surface-assisted laser desorption/ionization mass spectrometry imaging: A review. *Mass Spectrom. Rev.* 41: 373–420, 2022.

14) H. Huang, D. Ouyang, Z.-A. Lin. Recent advances in surface-assisted laser desorption/ionization mass spectrometry and its imaging for small molecules. *J. Anal. Test.* 6: 217–234, 2022.

15) H. Kawasaki, T. Ozawa, H. Hisatomi, R. Arakawa. Platinum vapor deposition surface-assisted laser desorption/ionization for imaging mass spectrometry of small molecules. *Rapid Commun. Mass Spectrom.* 26: 1849–1858, 2012.

16) T. Ozawa, I. Osaka, T. Ihozaki, S. Hamada, Y. Kuroda, T. Murakami, A. Miyazato, H. Kawasaki, R. Arakawa. Simultaneous detection of phosphatidylcholines and glycerolipids using matrix-enhanced surface-assisted laser desorption/ionization-mass spectrometry with sputter-deposited platinum film. *J. Mass Spectrom.* 50: 1264–1269, 2015.

17) T. Ozawa, I. Osaka, S. Hamada, T. Murakami, A. Miyazato, H. Kawasaki, R. Arakawa. Direct imaging mass spectrometry of plant leaves using surface-assisted laser desorption/ionization with sputter deposited platinum film. *Anal. Sci.* 32: 587–591, 2016.

18) R. Takata, Y. Nakabayashi, K. Hashimoto, A. Miyazato, I. Osaka. Imaging analysis of phosphatidylcholines and diacylglycerols using surface-assisted laser desorption/ionization mass spectrometry with metal film formed by mist chemical vapor deposition. *Mass Spectrom. (Tokyo)* 12: A0135, 2023.

19) H. Sato, S. Nakamura, K. Teramoto, T. Sato. Structural characterization of polymers by MALDI spiral-TOF mass spectrometry combined with Kendrick mass defect analysis. *J. Am. Soc. Mass Spectrom.* 25: 1346–1355, 2014.

20) K. De Bruycker, A. Welle, S. Hirth, S. J. Blanksby, C. Barner-Kowollik. Mass spectrometry as a tool to advance polymer science. *Nat. Rev. Chem.* 4: 257–268, 2020.

21) H. Sato, S. Nakamura, T. Fouquet, T. Ohmura, M. Kotani, Y. Naito. Molecular characterization of polyethylene oxide-based oligomers by surface-assisted laser desorption/ionization mass spectrometry using a through-hole alumina membrane as active substrate. *Rapid Commun. Mass Spectrom.* 34: e8597, 2020.

22) N. Dorival-García, F. Galbiati, R. Kruell, R. Kovasy, S. O. Dunne, K. D'Silva, J. Bones. Identification of additives in polymers from single-use bioprocessing bags by accelerated solvent extraction and ultra-high performance liquid chromatography coupled with high-resolution mass spectrometry. *Talanta* 219: 121198, 2020.

23) E. Blázquez-Blázquez, M. L. Cerrada, R. Benavente, E. Pérez. Identification of additives in polypropylene and their degradation under solar exposure studied by gas chromatography-mass spectrometry. *ACS Omega* 5: 9055–9063, 2020.

24) A. A. Cuthbertson, C. Lincoln, J. Miscall, L. M. Stanley, A. K. Maurya, A. S. Asundi, C. J. Tassone, N. A. Rorrer, G. T. Beckham. Characterization of polymer properties and identification of additives in commercially available research plastics. *Green Chem.* 26: 7067–7090, 2024.

25) T. Satoh, H. Niimi, N. Kikuchi, M. Fujii, T. Seki, J. Matsuo. Solvent-free silver-nanoparticle surface-assisted laser desorption/ionization imaging mass spectrometry of the Irganox 1010 coated on polystyrene. *Int. J. Mass Spectrom.* 404: 1–7, 2016.

26) K. Harata, S. Kitagawa, Y. Iiguni, H. Ohtani. Identification of polymer species in a complex mixture by pyrolysis-gas chromatography-atmospheric pressure chemical ionization-high resolution time-of-flight mass spectrometry as a basis for environmental microplastic analysis. *J. Anal. Appl. Pyrolysis* 148: 104828, 2020.

27) L. Sørensen, A. S. Groven, I. A. Hovsbakken, O. Del Puerto, D. F. Krause, A. Sarno, A. M. Booth. UV degradation of natural and synthetic microfibers causes fragmentation and release of polymer degradation products and chemical additives. *Sci. Total Environ.* 755: 143170, 2021.

28) W. He, S. Liu, W. Zhang, K. Yi, C. Zhang, H. Pang, D. Huang, J. Huang, X. Li. Recent advances on microplastic aging: Identification, mechanism, influence factors, and additives release. *Sci. Total Environ.* 889: 164035, 2023.